Science of the Total Environment 633 (2018) 317–328

Contents lists available at ScienceDirect

Science of the Total Environment

journal homepage: www.elsevier.com/locate/scitotenv

April 2008 Saharan dust event: Its contribution to PM_{10} concentrations over the Anatolian Peninsula and relation with synoptic conditions

B. Kabatas [a,c,*], R.B. Pierce [b], A. Unal [a], M.J. Rogal [c], A. Lenzen [c]

[a] Istanbul Technical University, Eurasia Institute of Earth Sciences, Istanbul, Turkey
[b] NOAA/NESDIS/STAR, USA
[c] University of Wisconsin-Madison, Space Science and Engineering Center, Madison, WI, USA

HIGHLIGHTS

- Utilizing high-resolution model improves the representation of mesoscale dynamics and reduces surface PM_{10} biases.
- Errors in synoptic transport cause an overestimation in surface PM_{10} by moving the dust plume faster than the observed.
- Modeled AODs are often not correlated with modeled surface concentrations, negative correlations occur due to aerosol aloft.

GRAPHICAL ABSTRACT

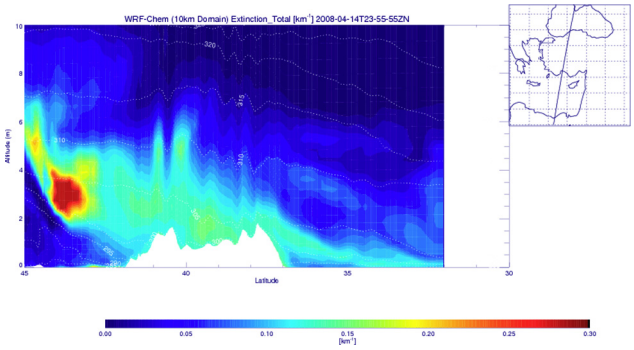

ARTICLE INFO

Article history:
Received 26 October 2017
Received in revised form 19 February 2018
Accepted 14 March 2018
Available online xxxx

Editor: P. Kassomenos

Keywords:
Saharan dust
WRF-Chem
HTAP
Air quality
Eastern Mediterranean

ABSTRACT

An online-coupled regional Weather Research and Forecasting model with chemistry (WRF-Chem) is utilized incorporating $0.1° \times 0.1°$ spatial resolution HTAP (Hemispheric Transport of Air Pollution) anthropogenic emissions to investigate the spatial and temporal distribution of a Saharan dust outbreak, which contributed to high levels (>50 μg/m^3) of daily PM_{10} concentrations over Turkey in April 2008. Aerosol optical depth and cloud optical thickness retrievals from the Moderate Resolution Imaging Spectroradiometer (MODIS) sensor on board of Aqua satellite are used to better analyze the synoptic conditions that generated the dust outbreak in April 2008. A "Sharav" low pressure system, which transports the dust from Saharan source region over Turkey along the cold front, tends to move faster in WRF-Chem simulations than observed. This causes the predicted dust event to arrive earlier than observed leading to an overestimation of surface PM_{10} concentrations in WRF-Chem simulation at the beginning of the event.

1. Introduction

Air pollution is one of the main threats on human health (Nel, 2005), ecology (Grantz et al., 2003) and climate (Fuzzi et al., 2015). The World Health Organization (WHO) states that particulate matter (PM) has more negative impacts on people than other pollutants and mineral dust is one of the largest components of PM. In a study conducted by Engelstaedter et al. (2006) the Saharan Desert is found to be the major contributor to the global dust budget with an estimated annual dust emission ranging between 130 and 760 Tg yr^{-1} while global dust emission estimates range from 1000 to 3000 Tg yr^{-1}. In another study, Tanaka and Chiba (2006) suggested that Sahara dust is responsible for

* Corresponding author at: University of Wisconsin-Madison, Space Science and Engineering Center, Madison, WI, USA.
E-mail address: kabatas@wisc.edu (B. Kabatas).

https://doi.org/10.1016/j.scitotenv.2018.03.150

>50% of the total global dust emissions. In their study, Kaufman et al. (2005) found that 240 ± 80 Tg of African dust is transported every year over the Atlantic Ocean reaching every corner of the globe. 20 Tg follows a transport route towards Africa and Europe at 30N–50N, including Mediterranean. Air pollution is considered as one of the main environmental threats in the Mediterranean Basin, since it is the crossroad of air masses transporting from Europe, Asia, Africa, and Middle East (Lelieveld et al., 2002). In addition to intercontinental transport of natural pollution sources from North Africa and anthropogenic emission sources from Europe, local emissions also have significant effects on air pollution levels in the Mediterranean Basin and air quality limits are often exceeded (Kanakidou et al., 2011; Paschalidou et al., 2015).

Atmospheric modeling helps us to understand the complex nature of aerosol formation and its impact on air quality. In the atmosphere, both meteorological parameters and chemical processes play important roles in air quality. Chemistry can influence the meteorology directly by influencing the radiation budget or indirectly by modifying the aerosol-cloud interactions. Meteorological parameters such as clouds, winds and precipitation also affect chemical transformation, transport and removal processes. The differences between online and offline air quality modeling methodologies were tested by Grell et al. (2004). Analysis of meteorological factors and chemical profiles showed that offline simulations are likely to have less accuracy in the vertical mass distribution compared to online modeling. Trace gases and particulates can be simulated at the same time step with the meteorological fields by a fully coupled "online" Weather Research and Forecasting/Chemistry model (WRF-Chem), a version of the non-hydrostatic model WRF (Skamarock et al., 2001). The meteorological and air quality components are fully consistent with each other since they use the same time step and transport scheme, as well as the same horizontal and vertical components of the grid (Grell et al., 2005; Fast et al., 2006).

Numerous studies have used WRF-Chem to understand a broad range of atmospheric chemistry issues (Tie et al., 2007; Tie et al., 2013; Chen et al., 2013; Kumar et al., 2012; Sessions et al., 2011; Follette Cook et al., 2015). However, only a few studies have been conducted that focus on natural dust related problems. Khan et al. (2015) utilized WRF-Chem to simulate the meteorological fields and the size distribution of the dust over northwest Africa in order to explore microphysical, and chemical properties of the Saharan dust. They found that orographic lifting, and land sea breeze interactions are the key mechanisms for aerosol plume formation. In another study, WRF-Chem was used to explain the seasonal and inter-annual variations of Asian dust balance, its direct radiative forcing, and estimates of the dust lifecycle contributions from transport, and dry and wet deposition (Chen et al., 2014). They showed that the WRF-Chem model was successful in simulating overall characteristics of mineral dust over the dust source region and dust direct radiative forcing, which resulted in atmospheric warming, with surface and TOA (top of atmosphere) cooling over East Asia. Kumar et al. (2014) used WRF-Chem to simulate the spatial and temporal distributions of dust plumes over northern India. The results showed an underestimation of Aerosol Optical Depth (AOD) compared to the AOD values obtained from AERONET (AErosol RObotic NETwork) sites. AERONET is a network of ground-based aerosol remote sensing that measure atmospheric aerosol properties (Holben et al., 1998).

In this current study, the Goddard Chemistry Aerosol Radiation and Transport (GOCART) bulk aerosol scheme (Chin et al., 2002) is used to represent atmospheric aerosol processes. This bulk approach, which represents the aerosols by total mass, is considered the simplest way to account for aerosols in numerical models. The GOCART aerosol scheme only accounts size information for dust and sea salt aerosols, and does not represent internally mixed aerosols, so there is no representation of particle coagulation processes in the model (Baklanov et al., 2014). The GOCART simple aerosol scheme (chem_opt = 300) does not include ozone chemistry, and PM_{10} is determined from GOCART only. There are also other more complex aerosol schemes available within WRF-CHEM model such as modal (MADE/SORGAM), and sectional (MOSAIC) schemes. However, we used GOCART bulk scheme due to its computational and numerical efficiency.

Literature studies show that the Saharan dust outbreaks more frequently occur in the Mediterranean Basin during the spring and fall transition seasons (Rodríguez et al., 2001; Gerasopoulos et al., 2006; Kallos et al., 2007; Mitsakou et al., 2008; Querol et al., 2009). Sahara dust transport into the Mediterranean Basin in the spring months is driven by intense baroclinic systems called Sharav cyclones (Meloni et al., 2007; Nastos, 2012). These cyclones develop downwind and to the south of the Atlas Mountains (which stretch through Morocco, Algeria and Tunisia, see Fig. 3 [10°W–10°E; 30°–35°N]) due to the convergence of cold marine air from the Atlantic and warm continental air (Alpert and Ziv, 1989). Dust mobilization occurs within the frontal region of these depressions due to the strong (>10 m s^{-1}) but steady winds along the coastal thermal gradient. These cyclones tend to move eastward along the southern coast of the Mediterranean Sea transporting dust over long distances towards the Eastern Mediterranean (Alpert and Ziv, 1989; Moulin et al., 1998; Barkan et al., 2005).

Previously, we utilized the Real-time Air Quality Modeling System (RAQMS) (Pierce et al., 2007), which includes assimilation of satellite AOD retrievals, to investigate the possible impacts of Saharan dust on Turkey's air quality in April 2008. The RAQMS model was found to overestimate the surface PM_{10} over Turkey by up to a factor of 5 (Kabatas et al., 2014). We hypothesized that this over estimate was due to its coarse resolution (2 × 2°) and inability to resolve local topographic variations. In this study, a series of higher resolution online-coupled regional WRF-Chem model simulations, driven by RAQMS lateral boundary conditions (LBC), are used to test this hypothesis. A 0.1° × 0.1° spatial resolution Hemispheric Transport of Air Pollution (HTAP) emission inventory (Janssens-Maenhout et al., 2012) is also incorporated into WRF-Chem and the updated model is utilized to investigate the spatial and temporal distribution of Saharan mineral dust transport over the Eastern Mediterranean for April 2008. This is the first WRF-Chem study investigating natural dust influences on air quality in the Anatolian Peninsula.

2. Data and methodology

2.1. Ground observations

The ground observations used in this study are obtained from the Turkish Ministry of Environment and Urbanization, which have been described and analyzed previously by Kabatas et al. (2014). The analysis of surface PM_{10} concentrations at the Turkey ground sites showed that the maximum mean daily PM_{10} concentration occurred on April 14, 2008 with a value of ~170 μg/m^3, which was also the maximum daily mean PM_{10} concentration measured throughout 2008 (Fig. 1).

The previous RAQMS analysis, along with Cloud-Aerosol Lidar and Infrared Pathfinder Satellite Observations (CALIPSO) (Winker et al., 2007), Terra and Aqua MODIS AOD observations showed that high levels of PM10 observed in April 2008 were found to be related to the long range transport of Saharan dust over Turkey (Kabatas et al., 2014).

2.2. Model description

The comparison of the previous 2 × 2 degree Real-Time Air Quality Modeling System (RAQMS) model to ground observations is shown in Fig. 2. The scatterplot is colored by the density of the data points. The statistical analysis shows the correlation between RAQMS model and the ground observations is 0.45, and that RAQMS overestimates the ground observations with model high biases of 232.5 μg/m^3.

In this study, we use RAQMS to provide LBC for WRF-Chem nested simulations (30 km outer and 10 km nested domains) to investigate the impact of model resolution on the spatial and temporal distribution of Saharan mineral dust transport over Eastern Mediterranean in April

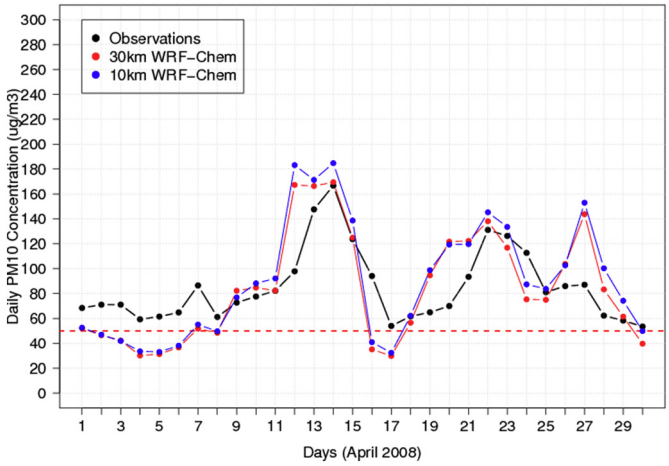

Fig. 1. Time series comparisons of ground observations (black), 30 km WRF-Chem (red) and 10 km WRF-Chem (blue) simulations. Red dashed line indicates the European Commission's daily air quality standard.

2008. Fig. 3 shows both 30 km and 10 km domains on top of a map showing terrain height.

GOCART (Chin et al., 2000) simulates five major tropospheric aerosol types including sea salt, dust, sulfate, and hydrophilic and hydrophobic components of black (BC) and organic (OC) carbon. GOCART module represents emission, advection, convection, and total deposition that determine each aerosol species' evolution. Dust emission is determined as a function of surface wind speed, and surface wetness. Sea salt emission is mainly a function of wind speed at 10 m, similar to dust uplifting (Chin et al., 2000, 2002; Ginoux et al., 2001). In this study, the size distribution is modeled into five size bins for dust (0.73–8.0 μm), and four size bins for sea salt (0.3–7.5 μm).

WRF-Chem supports high resolution (up to 4 km) anthropogenic emissions from the National Emissions Inventory (NEI) over the continental United States (CONUS), but uses low resolution (1° × 1°) Emission Database for Global Atmospheric Research (EDGAR) emissions for other regions. In order to improve the representation of the local emissions during the dust outbreak over Eastern Mediterranean, a higher resolution EDGAR anthropogenic emission inventory developed in cooperation with the Task Force on Hemispheric Transport of Air Pollution (TF HTAP) that consists monthly 0.1° × 0.1° global grids for year 2008 is

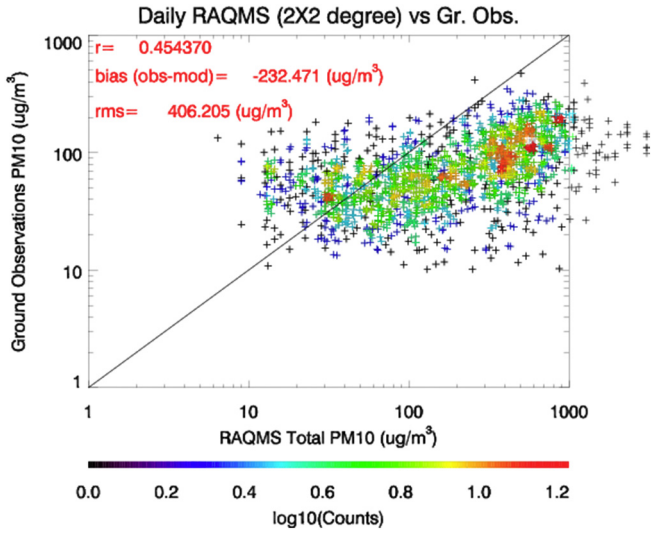

Fig. 2. Scatterplot for 2 × 2 degree RAQMS model and ground observations. Each color in the scatterplot represents the number of data points falling into each scatterplot bin.

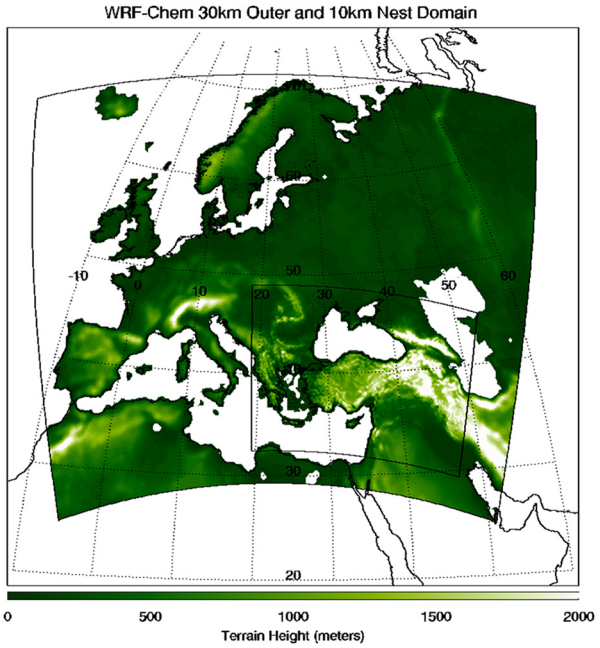

Fig. 3. WRF-Chem domains configured to cover Eastern Mediterranean (30 km outer domain) and Anatolian Peninsula (10 km inner domain) with topography map.

used. We combined EDGAR HTAP SO_2, OC, BC, PM_{10}, $PM_{2.5}$ emissions from Energy, Industry, Transport, and Residential sectors and replaced them in original EDGAR emission inventory to create higher resolution anthropogenic emissions over Eastern Mediterranean.

WRF-Chem biomass burning emissions uses Wild Fire Automated Biomass Burning Algorithm (WF-ABBA) wildfire detection (Prins and Menzel, 1994). For the region of this study, WF-ABBA fire detection and characterization from the Spinning Enhanced Visible and Infrared Imager (SEVIRI) onboard the Meteosat Second Generation (MSG) satellite were used to provide biomass burning emissions which were updated every 24 h.

The simulation presented here is associated with a dust storm that affected Eastern Mediterranean, especially Anatolian Peninsula, for April 2008. The outer WRF-Chem domain, with a horizontal resolution of 30 km, covers Europe in the west, Caspian Sea in the east, Scandinavia in the north and Sahara in the south (Fig. 3). WRF-Chem version 3.5.1 is configured to cover Eastern Mediterranean (−10.0°W–60.0°E, 30.0°S–70.0°N) with 190 west-east and 158 north-south grid points for the outer domain and 35 vertical layers up to 10 hPa. The high-resolution experiment has 10 km horizontal resolution, 262 west-east, 181 north-south grid points and the same 35 vertical layers as the 30 km outer domain.

The following physical parameterizations were used for both outer and nested runs: the Noah land surface model, Mellor-Yamada-Janjic Planetary Boundary Layer (PBL) (Janjić, 1994) and the Grell Cumulus Parameterization scheme. Meteorological fields are initialized and LBC are obtained from 6 hourly NOAA National Center for Environmental Prediction (NCEP) Global Forecast System (GFS) analyses. Aerosol LBC are obtained from 6 hourly RAQMS 2 × 2 degree global analyses. The simulation domain of this study does not cover North Africa, consequently, a significant portion of main dust source area is not included in the outer domain. However, by using 2 × 2 degree global RAQMS analysis, dust transport from North Africa is included through LBC. As noted previously, we compared RAQMS aerosol analyses with CALIPSO measurements to verify that RAQMS was able to capture the long range dust transport from its North African source region across the Mediterranean Sea (Kabatas et al., 2014). In order to account for

in-cloud rainout and below-cloud washout in large-scale precipitation, we set wet scavenging to "−10" (Grell, personal communication, December 2016) in the WRF-Chem name list. WRF-Chem was run in the above configuration for entire month of April 2008.

3. Results

Fig. 1 shows comparison of daily PM_{10} concentration of ground observations, WRF-Chem outer domain (30 km) and nested domain (10 km). The model daily mean prediction averaged over all ground observation sites (118 stations) is consistent with observations suggesting that the model captures the overall temporal evolution very well, yet all runs tend to overestimate the high values of PM_{10} (e.g. April 12, 2008) while they underestimate low PM_{10} events (e.g. April 16, 2008). It should be noted that the over prediction of WRF-Chem is much less than the RAQMS over prediction.

Fig. 4a, and b shows scatterplots of individual daily ground observations to the WRF-Chem outer domain (30 km), and WRF-Chem nested domain (10 km), respectively. As mentioned earlier, each color in the scatterplot represents the density of the data. The 30 km WRF-Chem run slightly underestimates the ground observations by 1.98 μg/m^3 while 10 km WRF-Chem run overestimates the ground observations by 2.86 μg/m^3. The correlation of 10 km run (0.477) is slightly higher than the 30 km run (0.467), and the root mean squared error of 30 km WRF-Chem run is smaller than WRF-Chem 10 km (62.64 μg/m^3, 65.13 μg/m^3, respectively).

Utilizing the WRF-Chem 30 km and 10 km forecasts instead of the 2 × 2 degree RAQMS analysis results in slight improvements in the correlation and significant reductions biases and RMSE (see Fig. 2). For the WRF-Chem simulations, we find that utilizing a higher resolution domain leads to changes in biases from low positive biases to slightly higher negative biases. The higher resolution WRF-Chem domain also adds more variance to the surface PM_{10} predictions, leading to the increase in RMSE values.

To assess the skill in predicting dust events, we separated the WRF-Chem forecasts into high and low dust events, defined by the dust mass fraction (ratio of dust to the total PM10 concentration). Correlations between ground observations from all 118-ground stations and 30 km WRF-Chem run is found to be 0.43 when the dust mass fraction is >50%, and 0.30 when the dust mass fraction is <50%. Correlations between ground observations and the 10 km WRF-Chem nested run is found to be 0.47 when dust fraction is over 50% and 0.29 when the dust fraction is <50%. This shows that the higher resolution 10 km domain improves the overall dust predictions compared to 30 km domain results during the dust event. This analysis also shows that neither WRF-Chem run can adequately predict the PM_{10} that is associated with the local emissions when dust is not the dominant aerosol, even with the higher resolution HTAP emission inventory used in this study.

Fig. 5a–c shows surface PM_{10} predictions for both WRF-Chem 30 km domain and 10 km domain and the observed PM_{10} and is used to understand the aerosol transport during the dust event. We focus on April 12, where both models overestimated the daily in situ measurements, April 14, where the models and in situ measurements have a good agreement, and April 16, 2008, where the models underestimated the daily in situ measurements (see Fig. 1). It should be noted that the ability to assess the gradient of surface PM_{10} concentration between west and east part of Turkey is affected by the representativeness of the positioning of ground-based air quality monitoring sites as well as their data availability.

Saharan dust dominates the whole region when it is transported from North Africa over the Mediterranean Sea to Turkey with surface values around 250 μg/m^3 (~2.4 $\log_{10}$) throughout the high dust event episode (11–18 April 2008). During the dust event, dust is transported from North Africa over the Mediterranean Sea to Turkey by southwesterly winds. For the first few days, dust intrusions affect the western part of Turkey as well as southern Italy and southeastern Balkans. On April 12, 2008 (Fig. 5a) dust reaches out to Anatolian peninsula, and it dominates the region on April 14, 2008 (Fig. 5b). For the rest of the episode, the Saharan dust cloud covers Turkey, moving towards eastern part of Turkey by the end of the episode. Towards the end of the episode (starting on April 16, 2008 (Fig. 5c)), clean continental air is transported from the northwest into the region.

4. Synoptic discussion

In April 2008, Sharav cyclone conditions favored Sahara dust to transport from North Africa over Mediterranean Basin to Anatolian peninsula. Both 30 km and 10 km WRF-Chem runs show good agreement with observed surface PM_{10} concentration on April 14, 2008, when the maximum PM_{10} concentration was observed with a daily mean value of 170 μg/m^3. However, the predicted dust increases begun a few days earlier (April 11, 2008) and declined sooner (April 16, 2008) than observed. On April 12, 2008, both WRF-Chem runs overestimate the ground observations, while they underestimate the ground observations towards the end of the episode on April 16, 2008. In order to investigate how errors in the predicted synoptic flow and the long-range transport of the mineral dust from Sahara to Turkey influence these predictions, we compared the observed and predicted synoptic patterns on

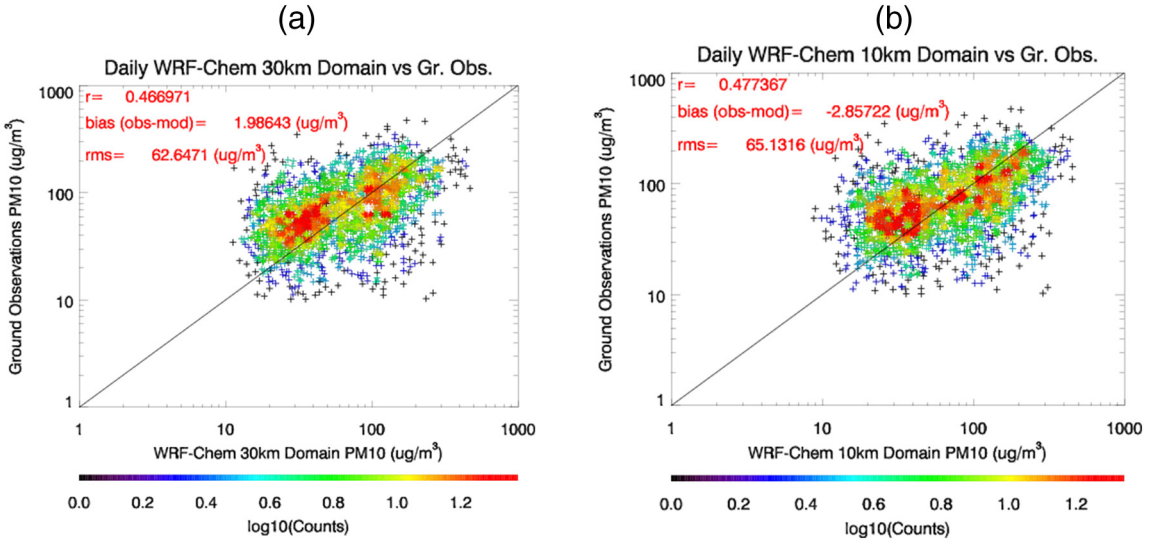

Fig. 4. Scatter plots for WRF-Chem outer (30 km horizontal resolution) (a), and nested (10 km horizontal resolution) (b), respectively.

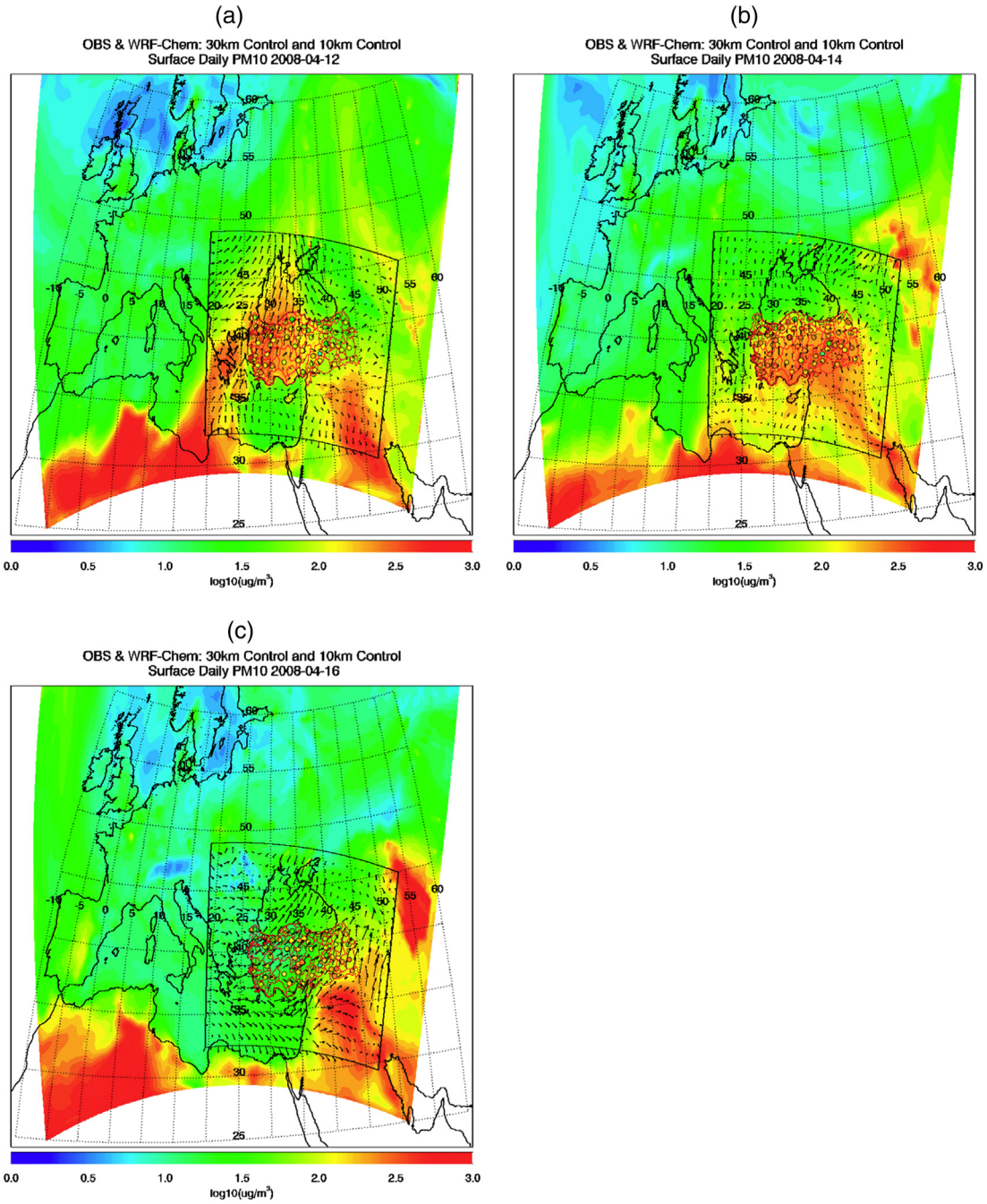

Fig. 5. WRF-Chem 30 km and 10 km daily surface PM_{10} concentration maps for April 12 (a), April 14 (b), and April 16 (c), 2008. Colored circles show the observed PM10 concentrations. Black arrows show 10-meter wind vectors for the WRF-Chem 10 km domain.

April 12, 14 and 16, 2008 in Figs. 6, 7, and 8, respectively. We use MODIS Cloud Optical Thickness (COT) retrievals and WRF-Chem COT predictions to characterize synoptic transport errors.

The first panel shows the mean sea level pressure along with the wind vectors obtained from the 30 km WRF-Chem simulation, the middle panel shows the WRF-Chem COT, and the right panel shows COT from MODIS Aqua cloud product (MYD06). Since the Aqua satellite passes over Turkey around noon, we show the comparison of predicted and analyzed COT at 12Z.

On April 11, at the beginning of the episode, the high pressure system over the North Africa is divided by a trough creating two separate high pressure centers. The trough centered near 30° N over Tunisia induces south and south-westerly winds, which, combined with the high pressure system over Eastern Mediterranean, creates a front that triggers a dust storm over Mediterranean Basin that originates from the Saharan source region. Another important synoptic feature at this time is the development of a second trough over Eastern Europe that continues to develop over the region, then deepens and moves towards northeast on April 12, 2008 (Fig. 6a).

The warm conveyor belt transports moist air northward from southern Mediterranean as the low pressure system moves eastward on April 12 (Fig. 6b). Southerly winds ahead of the cold front transports dust over the western part of Turkey on the same day. The cold front can also be seen from the MODIS COT retrieval on April 12, 2008 (Fig. 6c).

MODIS shows the cold front extending from Cap Bon (which is in far northeastern Tunisia) to the northwestern part of Sicily towards Italy.

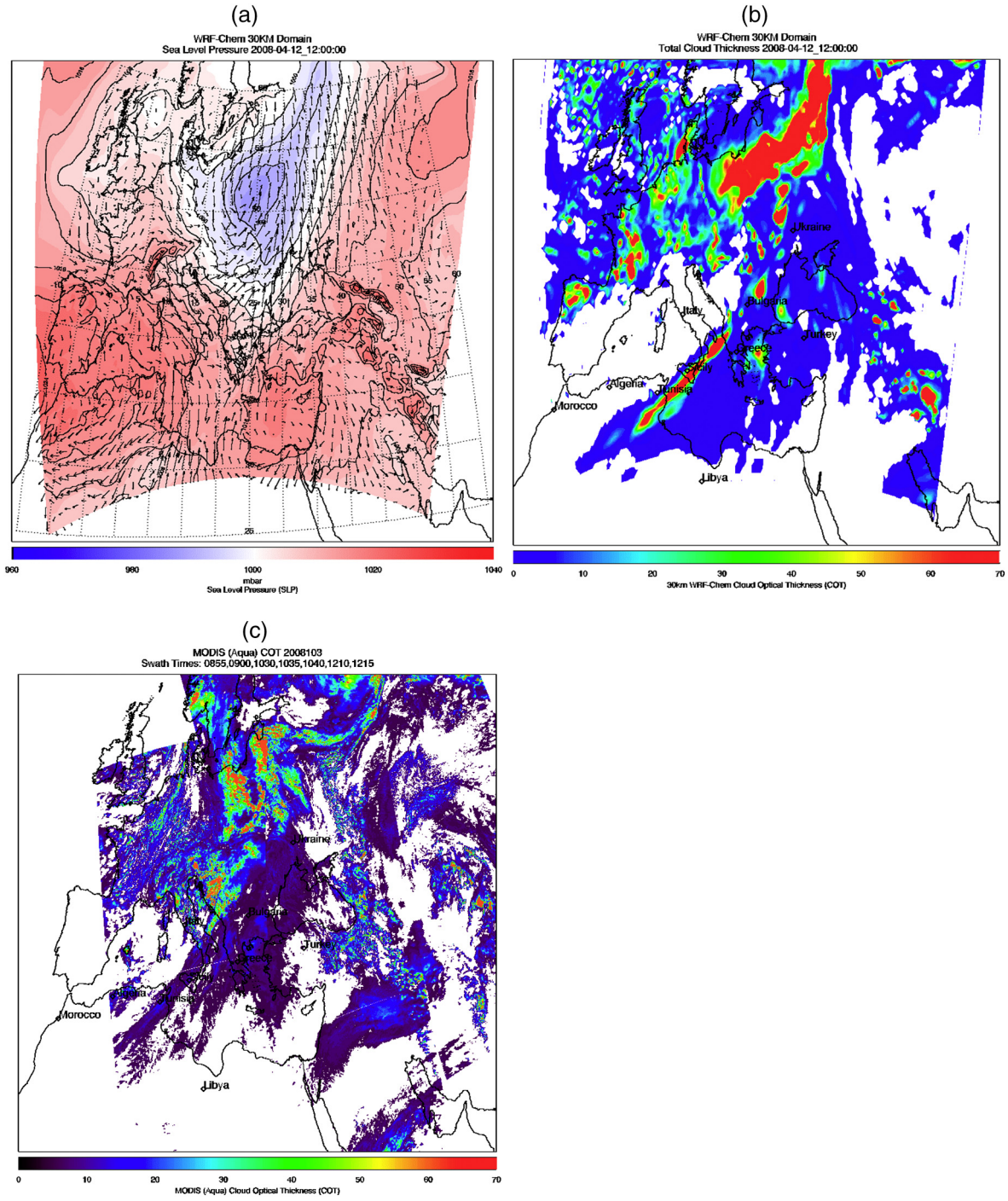

Fig. 6. Mean sea level pressure (a) and the cloud optical thickness maps from WRF-Chem (b) and Aqua MODIS cloud product (c) for April 12, 2008.

The WRF-Chem prediction shows cold front extending from the southern part of Cap Bon to the southeastern part of Sicily, indicating that the low pressure system moves faster in the WRF-Chem predictions than observed. As a result, the predicted arrival of the dust event over Turkey occurs earlier than observed leading to an overestimation of surface PM_{10} concentrations at the beginning of the event.

On April 14, the high pressure system fills in behind the cold front as the system moves towards northeastern part of Libya (Fig. 7a). On the warm side of the cold front, the warm conveyor belt curves anticyclonically showing a classic baroclinic leaf cloud formation over Balkan region that stretches from Bulgaria to the southern part of the Black Sea on April 14, 2008 (Fig. 7b). This is when the maximum dust concentrations occur over Anatolian Peninsula.

The predicted baroclinic leaf structure on April 14, 2008 is also apparent in the MODIS cloud retrievals as a curved band of clouds situated over Greece, stretching through Bulgaria and reaching to Ukraine and the northern part of Black sea (Fig. 7c). This pressure system continues moving towards the north and situates over northern part of the Black Sea on April 15, 2008. On April 16, the WRF-Chem simulation predicts that clean air is transported from the northwest into the region (Fig. 8a) as low pressure system moves eastward along the coast of northern Black Sea (Fig. 8b) while MODIS COT shows it as moving towards the north (Fig. 8c). This error in the predicted synoptic transport leads to an underestimation of surface PM_{10} concentrations at the end of the episode, due to transport of relatively clean continental air over Turkey sooner than was observed.

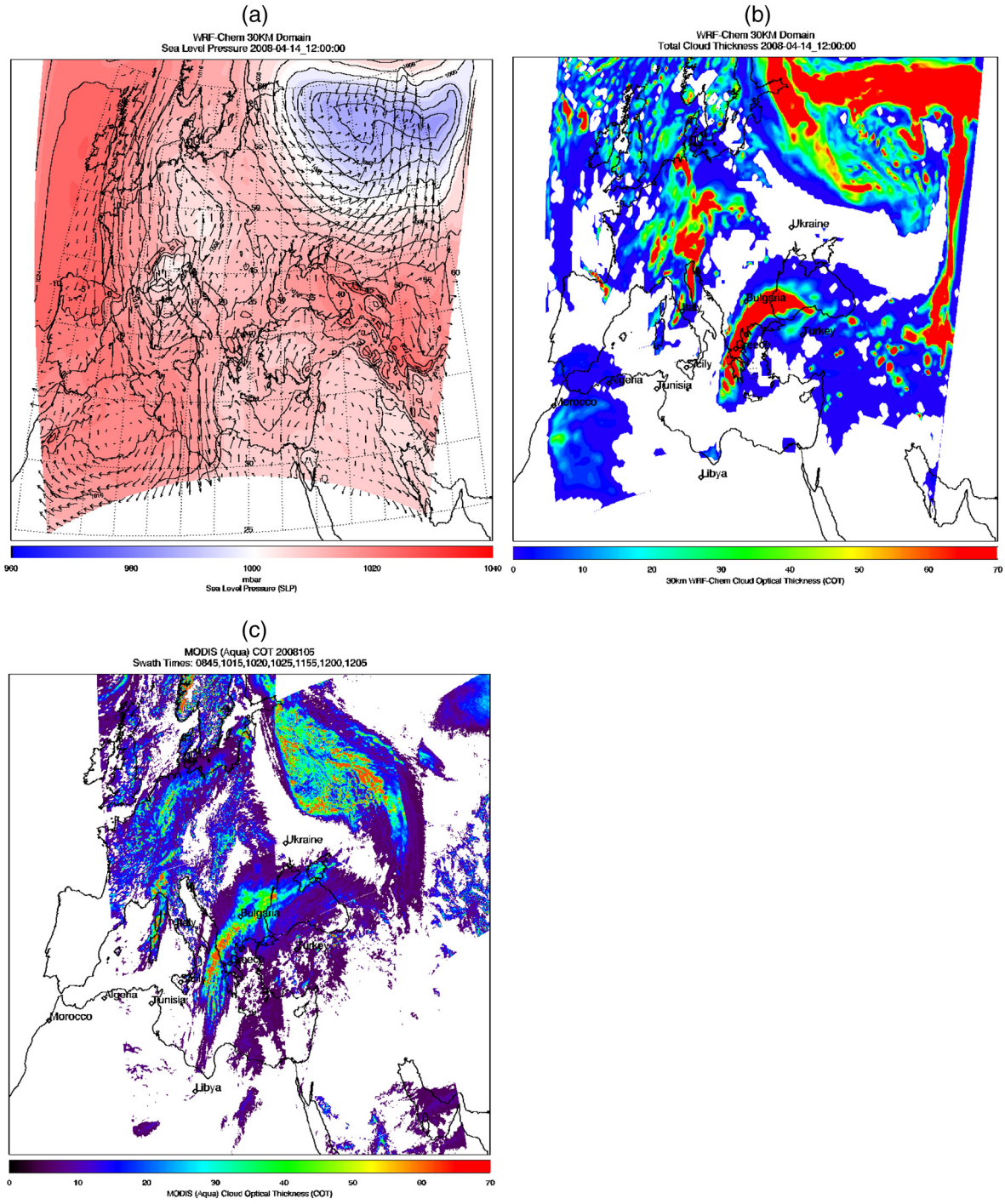

Fig. 7. Mean sea level pressure (a) and the total cloud thickness maps from WRF-Chem (b) and Aqua MODIS cloud product (c) for April 14, 2008.

5. Predicted aerosol optical depth

The Moderate Resolution Imaging Spectroradiometer (MODIS) Aerosol Product (MYD04 for Aqua), Collection 6, is used to obtain information about AOD at 550 nm, which represents columnar aerosol loading of the atmosphere. The MODIS aerosol algorithm consists of two different algorithms. The dark target algorithm derives aerosols over vegetated/dark-soiled land and ocean surfaces, while the deep blue algorithm derives aerosols covering cloud and snow free bright land surfaces like desert and arid lands (Hsu et al., 2004; Levy et al., 2013; Sayer et al., 2013). We use the combined retrieval in the following analysis. Fig. 9a and b shows the aerosol optical depth obtained from WRF-Chem and Aqua MODIS for April 14, 2008 at 12:00 UTC, respectively (Aqua overpasses Turkey around noon). AOD values within the dust cloud that is transported from North Africa over the Eastern Mediterranean vary from 0.7 and 1.0 for WRF-Chem, and 0.6 and 0.8 for Aqua MODIS. MODIS shows an optically thick aerosol layer over western part of Cyprus with values around 0.9, while WRF-Chem shows the AOD of 0.6 near Cyprus.

Sayer et al. (2013) showed that the MODIS retrieval performance varies regionally due to the overestimation of surface reflectance and differences in aerosol microphysical properties. Over the semi-arid/arid regions in Northern Africa, MODIS Deep Blue aerosol product had poorest performance and negative correlation when compared to

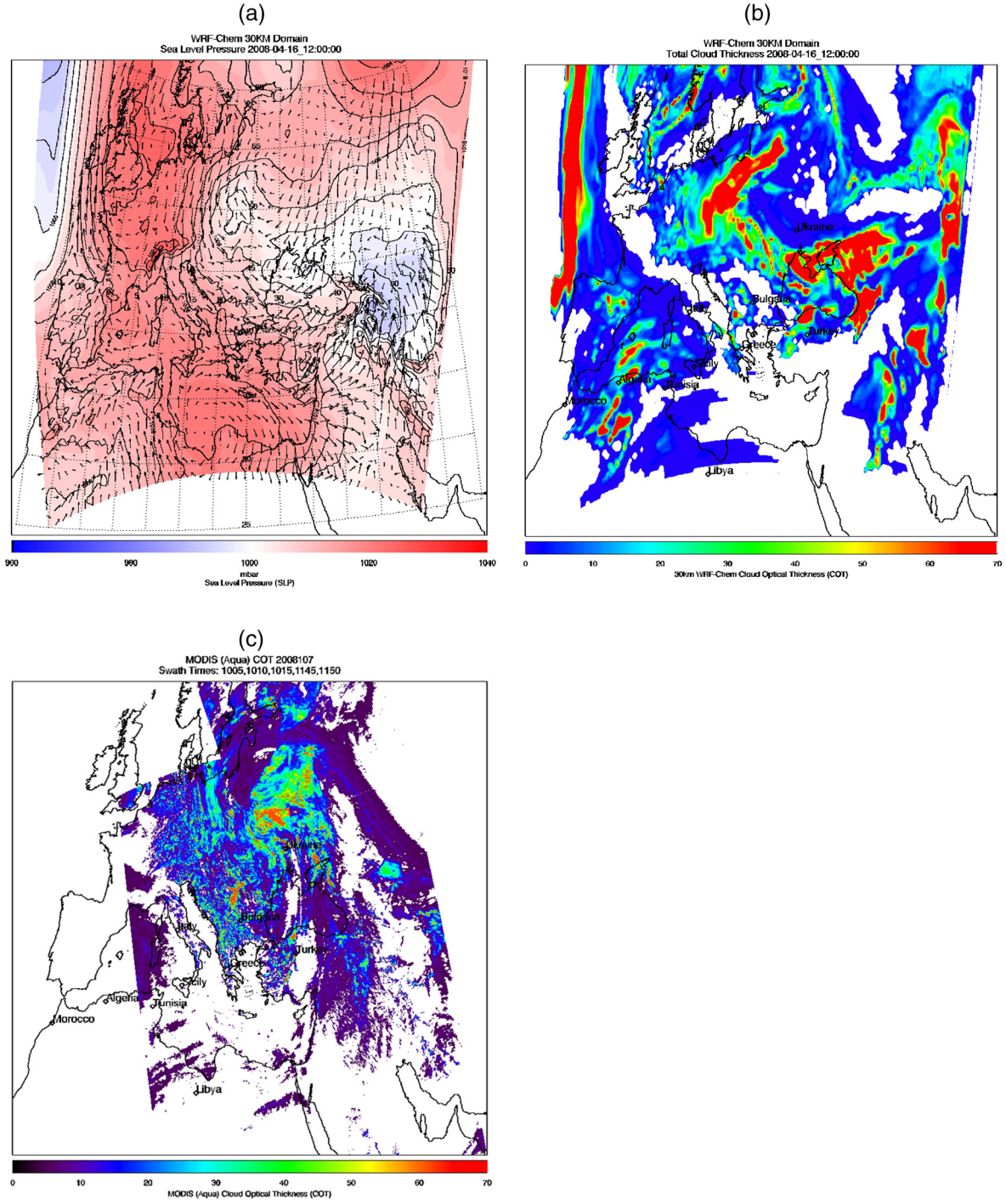

Fig. 8. Mean sea level pressure (a) and the total cloud thickness maps from WRF-Chem (b) and Aqua MODIS cloud product (c) for April 16, 2008.

AERONET stations. Over the ocean MODIS Dark Target aerosol product overestimates the AOD at 0.55 μm (Levy et al., 2013). In their review satellite aerosol observations, Hoff and Christopher (2009) focused on the approaches that were used to estimate the linear relationship between AOD and ground-level particulate matter (PM). They stated that by using satellite AOD, ±30% of the variance in surface $PM_{2.5}$ measurements can be estimated. The variability between AOD and PM depends on the region, time of the year, aerosol microphysical properties, and extrinsic properties like humidity and boundary layer height.

In our study, we use the WRF-Chem PM_{10} and AOD predictions to examine the correlation between AOD and surface PM_{10} for both 30 km and 10 km domains (Fig. 10). Comparisons between modeled AOD and surface PM_{10} show that AODs are generally slightly more positively correlated with the modeled surface PM_{10} concentrations in 10 km run than in 30 km run but are otherwise very similar. The high correlations during April 22–29, 2008 occur after the dust episode and are associated with aerosols from local emissions that remain within the boundary layer. The lowest correlations between modeled AODs and surface PM_{10} occur during the high dust event day (April 14, 2008) for both 30 km and 10 km runs.

We use CALIPSO aerosol extinction measurements to verify the vertical transport within the WRF-Chem aerosol prediction and demonstrate how the vertical distribution of the aerosol loading can influence the correlation between modeled AODs and surface PM_{10} on

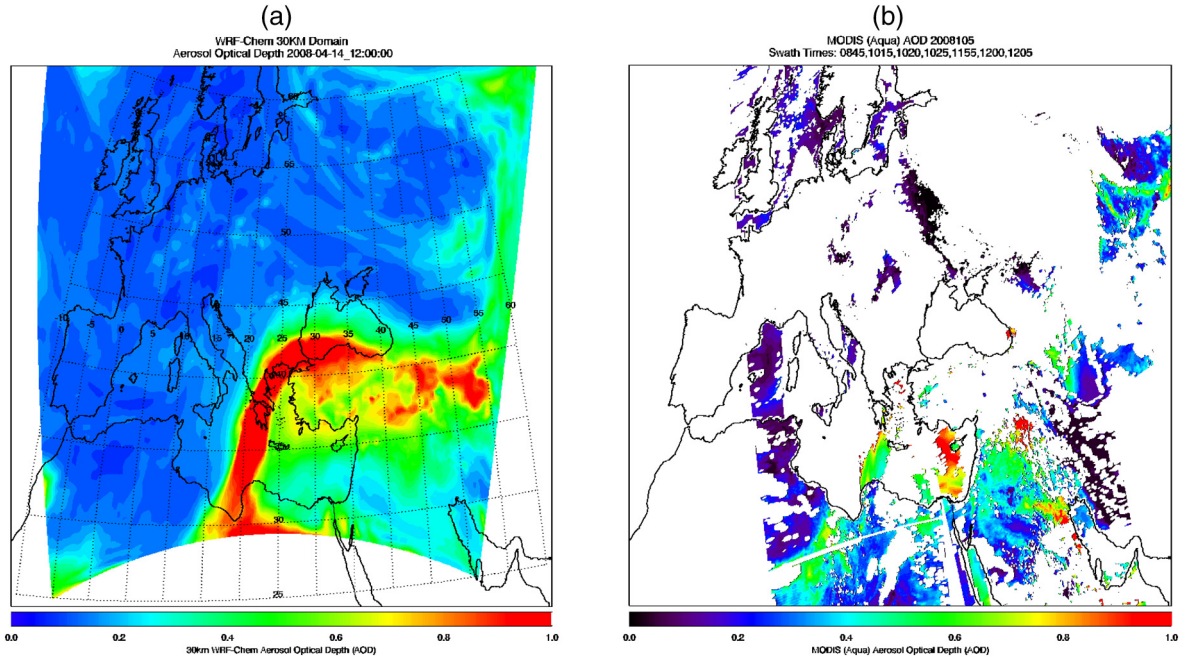

Fig. 9. AOD predicted from WRF-Chem (a), and obtained from Modis (b) MYD04 (Aqua) aerosol product for Eastern Mediterranean Basin for April 12, 2008.

April 14, 2008, when maximum daily surface PM10 concentration was observed. Fig. 11a, and b shows the measured and modeled total extinction cross sections along the CALIPSO orbital track that passed over Turkey at 23:55Z on April 14, 2008. CALIPSO (Fig. 11a) shows extinction enhancements below 2 km over the southern part of Turkey. High aerosol extinctions extend up to nearly 6 km over Turkey. WRF-Chem 30 km (Fig. 11b) and 10 km (Fig. 11c) analysis show a very similar aerosol extinction cross section with aerosol lifting over the Mediterranean Sea starting from the North African coast to the southern part of Turkey.

The layer of enhanced aerosol extinction reaches up to 5 km over Turkey as observed from CALIPSO data. This decoupling between the aerosol plume and the surface as the dust is transported over Turkey within the Sharav cyclone accounts for the lack of correlation between the modeled AOD and modeled surface PM_{10}. The comparison between two WRF-Chem runs shows that there is more aerosol lofting in the 10 km cross-section than the 30 km one, particularly over the mountains in the northern part of Turkey. The increased resolution of the topography can also be clearly seen in 10 km cross-section. The 10 km simulation also shows small-scale variations in the potential temperature cross sections that might be associated with orographic gravity waves (Lilly and Klemp, 1979), that are not resolved in the 30 km simulation. Vertical transport of the dust by these orographic gravity waves may account for the additional lofting found in the 10 km simulation. Unfortunately, the CALIPSO aerosol retrievals were obscured by clouds in this region and cannot be used to verify this orographic gravity wave signature.

In our previous study, RAQMS underestimated aerosol lofting over Turkey leading to overestimates in surface PM_{10}. The current study shows that this was likely due to poor representation of the sharp gradients in topography and land/sea temperatures that are necessary to simulate the dust transport over Turkey. Utilizing a higher resolution regional model has improved the representation of both synoptic and mesoscale dynamics which lead to the overestimation of surface PM_{10} in the 2×2 degree resolution RAQMS aerosol analysis.

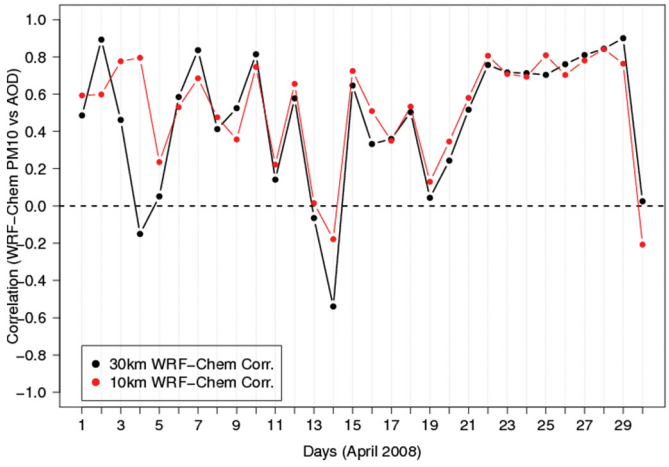

Fig. 10. Correlation between modeled AOD and Surface PM_{10} concentration for WRF-Chem 30 km (black) and 10 km (red) domain for April 2008.

6. Conclusion

In our previous study, RAQMS aerosol analyses were used to investigate the contribution of Saharan dust on high levels of PM_{10} observed over Turkey in April 2008. Results of the RAQMS experiment showed that the model over predicted the surface PM_{10} values by factor of 5, although it captured the overall trends in concentration patterns fairly well. In this research, we utilized an online-coupled WRF-Chem system to investigate spatial and temporal distribution of Saharan mineral dust transport over Eastern Mediterranean, using the RAQMS model to provide the lateral boundary conditions. This is the first WRF-Chem study investigating natural dust influences (dust and anthropogenic impact together) on air quality in the Eastern Mediterranean, especially in Anatolian Peninsula. The current results show significantly improved the representation of both synoptic and mesoscale dynamics compared to the previous study, however, synoptic transport errors remain.

The correlations between ground observations and the WRF-Chem 30 km and 10 km domain runs are 0.47 and 0.48, respectively. The 30 km WRF-Chem run underestimates the ground observations by 1.98 $\mu g/m^3$, while 10 km WRF-Chem run overestimates the ground

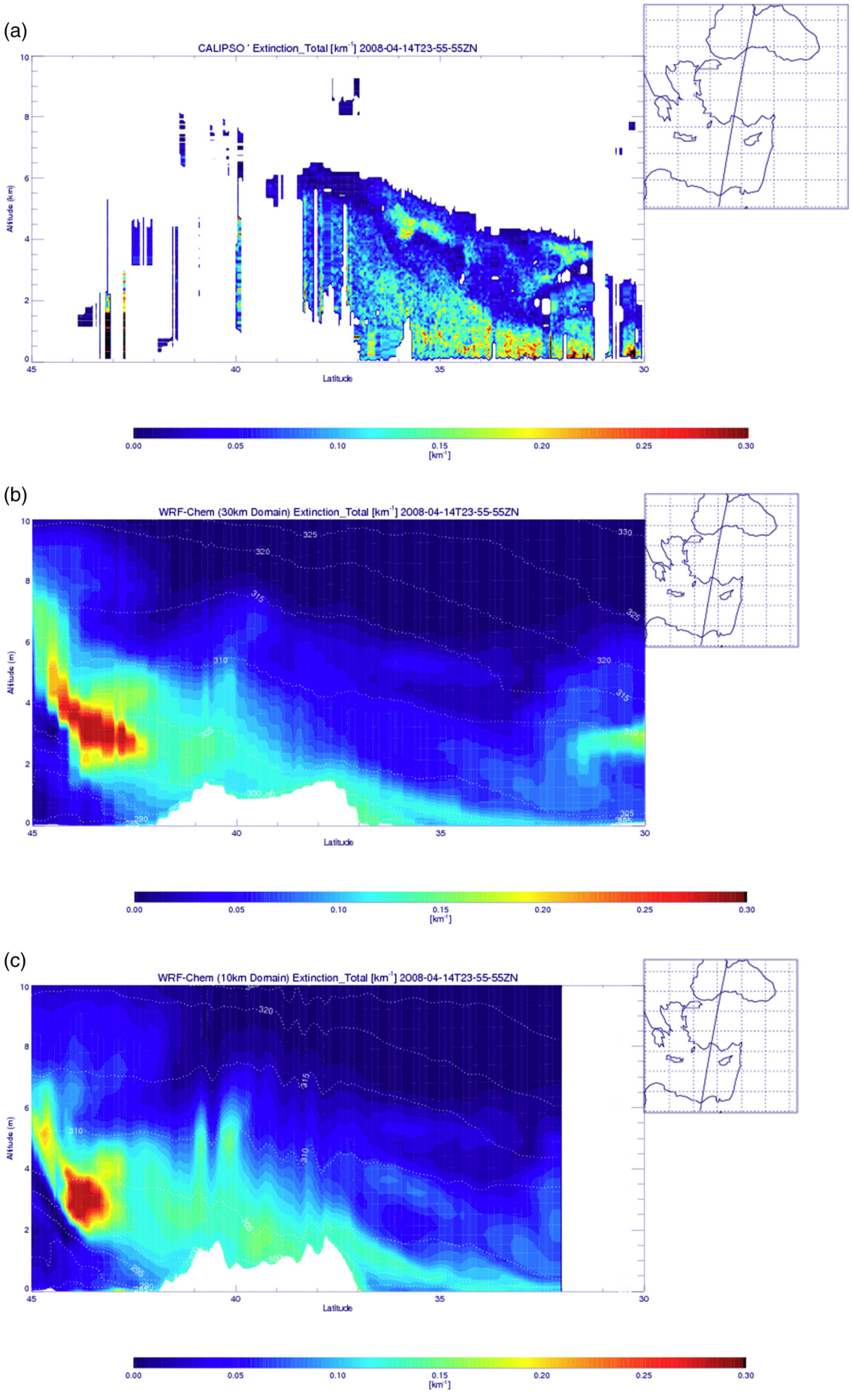
(a)
CALIPSO ' Extinction_Total [km-1] 2008-04-14T23-55-55ZN
Altitude (km)
Latitude
45
40
35
30
0.00
0.05
0.10
0.15
0.20
0.25
0.30
[km-1]
(b)
WRF-Chem (30km Domain) Extinction_Total [km-1] 2008-04-14T23-55-55ZN
Altitude (m)
Latitude
(c)
WRF-Chem (10km Domain) Extinction_Total [km-1] 2008-04-14T23-55-55ZN
Altitude (m)
Latitude

observations by 2.85 μg/m^3. Both WRF-Chem runs tend to overestimate the high PM_{10} events while they underestimate the low PM_{10} events.

In order to understand why WRF-Chem overestimated the surface PM_{10} levels at the beginning of the dust event, and underestimated it towards the end of the episode, MODIS AOD and cloud optical thickness (COT) were used to evaluate the model predictions of synoptic transport. Analysis suggests that the Sharav cyclone, which transports dust from source area over Turkey along the cold front, tends to move faster across the Mediterranean in the WRF-Chem predictions than observed. This causes the dust event to arrive over Turkey earlier than the observations leading to an overestimation of surface PM_{10} concentrations in WRF-Chem simulation at the beginning of the event (April 12, 2008). Towards the end of the episode, the WRF-Chem prediction brings clean continental air from the northwest into the region and sweeps the dust out to the east along the northern coast of the Black Sea, while MODIS shows the system moving to the north. This error in synoptic transport leads to an underestimation of surface PM_{10} concentrations at the end of the event (April 16, 2008).

The comparison between modeled AOD and surface PM_{10} showed that the AODs are highly correlated with the surface PM_{10} concentrations in both 10 km and 30 km runs during some periods and not during others. The negative correlations from both runs on April 14, 2008 occur due to lofting of the aerosols. Both CALIPSO and WRF-Chem show similar vertical distribution of aerosol over Turkey suggesting that aerosol lifting over the peninsula leads to a decoupling between the aerosol loading and surface concentrations on April 14, 2008.

In this research, we considered dust over the Anatolian peninsula at two different domains (30 km and 10 km horizontal resolution). Results showed that while there was significant improvement in the agreement with surface PM_{10} observations between the 30 km WRF-Chem prediction and the previous 2 × 2 degree RAQMS aerosol analysis, there is no significant improvement when a higher resolution (10 km) domain is employed over Turkey. The study demonstrates that the approaches presented here are useful tools to investigate the meteorological conditions that lead to dust transport and its impact on air quality, but errors in synoptic transport remain and need to be reduced to accurately predict the exact timing of the events.

Acknowledgement

We would like to thank Liam E. Gumley for his support. This study was supported in part by NASA (National Aeronautics and Space Administration) project NNG15HZ38C and TUBITAK (Scientific and Technological Research Council of Turkey) grant number 111G037. The views, opinions, and findings contained in this report are those of the author(s) and should not be construed as an official National Oceanic and Atmospheric Administration or U.S. Government position, policy, or decision.

References

Alpert, P., Ziv, B., 1989. The Sharav cyclone—observations and some theoretical considerations. J. Geophys. Res. 94, 18495–18514.
Baklanov, A., Schlünzen, K., Suppan, P., Baldasano, J., Brunner, D., Aksoyoglu, S., ... Zhang, Y., 2014. Online coupled regional meteorology chemistry models in Europe: current status and prospects. Atmos. Chem. Phys. 14:317–398. https://doi.org/10.5194/acp-14-317-2014.
Barkan, J., Alpert, P., Kutiel, H., Kishcha, P., 2005. Synoptics of dust transportation day from Africa toward Italy and central Europe. J. Geophys. Res. 110, 208.
Chen, D., Li, Q., Stutz, J., Mao, Y., Zhang, L., Pikelnaya, O., Tsai, J., 2013. WRF-Chem simulation of NOx and O_3 in the LA Basin during CalNex 2010. Atmos. Environ. 81, 421–432.
Chen, S., Zhao, C., Qian, Y., Leung, L.R., Huang, J., Huang, Z., ... Li, J., 2014. Regional modeling of dust mass balance and radiative forcing over East Asia using WRF-Chem. Aeolian Res. 15, 15–30.
Chin, M., Rood, R.B., Lin, S.J., Müller, J.F., Thompson, A.M., 2000. Atmospheric sulfur cycle simulated in the global model GOCART: model description and global properties. J. Geophys. Res. 105, 24671–24687.
Chin, M., Ginoux, P., Kinne, S., Torres, O., Holben, B.N., Duncan, B.N., ... Nakajima, T., 2002. Tropospheric aerosol optical thickness from the GOCART model and comparisons with satellite and Sun photometer measurements. J. Atmos. Sci. 59, 461–483.
Engelstaedter, S., Tegen, I., Washington, R., 2006. North African dust emissions and transport. Earth Sci. Rev. 79, 73–100.
Fast, J.D., Gustafson Jr., W.I., Easter, R.C., Zaveri, R.A., Bernard, J.C., Chapman, E.G., Grell, G.A., Peckham, S.E., 2006. Evolution of ozone, particulates, and aerosol direct radiative forcing in the vicinity of Houston using a fully coupled meteorology-chemistry-aerosol model. J. Geophys. Res. 111:D21305. https://doi.org/10.1029/2005JD006721.
Follette Cook, M.B., Pickering, K.E., Crawfordi, J.H., Duncan, B.N., Loughner, C.P., Diskin, G.S., Fried, A., Weinheimer, A.J., 2015. Spatial and temporal variability of trace gas columns derived from WRF/Chem regional model output: planning for geostationary observations of atmospheric composition. Atmos. Environ. 118:28–44. https://doi.org/10.1016/j.atmosenv.2015.07.024.
Fuzzi, S., Baltensperger, U., Carslaw, K., Decesari, S., Denier van der Gon, H., Facchini, M.C., Gilardoni, S., 2015. Particulate matter, air quality and climate: lessons learned and future needs. Atmos. Chem. Phys. 15, 8217–8299.
Gerasopoulos, E., Kouvarakis, G., Babasakalis, P., Vrekoussis, M., Putaud, J.P., Mihalopoulos, N., 2006. Origin and variability of particulate matter (PM_{10}) mass concentrations over the Eastern Mediterranean. Atmos. Environ. 40, 4679–4690.
Ginoux, P., Chin, M., Tegen, I., Prospero, J., Holben, B., Dubovik, O., Lin, S.J., 2001. Sources and distributions of dust aerosols simulated with the GOCART model. J. Geophys. Res. 106, 20225–20273.
Grantz, D.A., Garner, J.H.B., Johnson, D.W., 2003. Ecological effects of particulate matter. Environ. Int. 29, 213–239.
Grell, G. A., 2016. Personal communication.
Grell, G.A., Knoche, R., Peckham, S.E., McKeen, S.A., 2004. Online versus offline air quality modeling on cloud-resolving scales. Geophys. Res. Lett. 31, L16117. https://doi.org/10.1029/2004GL020175.
Grell, G.A., Peckham, S.E., Schmitz, R., McKeen, S.A., Frost, G., Skamarock, W.C., Eder, B., 2005. Fully coupled "online" chemistry within the WRF model. Atmos. Environ. 39, 6957–6975.
Hoff, R.M., Christopher, S.A., 2009. Remote sensing of particulate pollution from space: have we reached the promised land? J. Air Waste Manage. Assoc. 59, 645–675.
Holben, B.N., et al., 1998. AERONET—A federated instrument network and data archive for aerosol characterization. Remote Sens. Environ. 66, 1–16.
Hsu, N.C., Tsay, S.C., King, M.D., Herman, J.R., 2004. Aerosol properties over bright-reflecting source regions. IEEE Trans. Geosci. Remote 42, 557–569.
Janjić, Z.I., 1994. The step-mountain eta coordinate model: further developments of the convection, viscous sublayer, and turbulence closure schemes. Mon. Weather Rev. 122, 927–945.
Janssens-Maenhout, G., Dentener, F., van Aardenne, J., Monni, S., Pagliari, V., Orlandini, L., ... Keating, T., 2012. EDGAR-HTAP: A Harmonized Gridded Air Pollution Emission Dataset Based on National Inventories.
Kabatas, B., Unal, A., Pierce, R.B., Kindap, T., Pozzoli, L., 2014. The contribution of Saharan dust in PM10 concentration levels in Anatolian Peninsula of Turkey. Sci. Total Environ. 488–489, 413–421.
Kallos, G., Astitha, M., Katsafados, P., Spyrou, C., 2007. Long-range transport of anthropogenically and naturally produced particulate matter in the Mediterranean and North Atlantic: current state of knowledge. J. Appl. Meteorol. Climatol. 46, 1230–1251.
Kanakidou, M., Mihalopoulos, N., Kindap, T., Im, U., Vrekoussis, M., Gerasopoulos, E., ... Moubasher, H., 2011. Megacities as hot spots of air pollution in the East Mediterranean. Atmos. Environ. 45, 1223–1235.
Kaufman, Y.J., Koren, I., Remer, L.A., Tanre, D., Ginoux, P., Fan, S., 2005. Dust transport and deposition observed from the Terra MODIS spacecraft over the Atlantic Ocean. J. Geophys. Res. 110:D10S12. https://doi.org/10.1029/2003JD004436.
Khan, B., Stenchikov, G., Weinzierl, B., Kalenderski, S., Osipov, S., 2015. Quantifying dust plume formation and aerosol size distribution during the Saharan Mineral Dust Experiment in North Africa. Tellus B 67:1. https://doi.org/10.3402/tellusb.v67.27170.
Kumar, R., Naja, M., Pfister, G.G., Barth, M.C., Wiedinmyer, C., Brasseur, G.P., 2012. Simulations over South Asia using the Weather Research and Forecasting model with Chemistry (WRFChem): chemistry evaluation and initial results. Geosci. Model Dev. 5: 619–648. https://doi.org/10.5194/gmd-5-619-2012.
Kumar, R., Barth, M.C., Pfister, G.G., Naja, M., Brasseur, G.P., 2014. WRF-Chem simulations of a typical pre-monsoon dust storm in northern India: influences on aerosol optical properties and radiation budget. Atmos. Chem. Phys. 14:2431–2446. https://doi.org/10.5194/acp-14-2431-2014.
Lelieveld, J., Berresheim, H., Borrmann, S., Crutzen, P.J., Dentener, F.J., Fischer, H., ... Ziereis, H., 2002. Global air pollution crossroads over the Mediterranean. Science 298, 794–799.
Levy, R.C., Mattoo, S., Munchak, L.A., Remer, L.A., Sayer, A.M., Patadia, F., ... Hsu, N.C., 2013. The Collection 6 MODIS aerosol products over land and ocean. Atmos. Meas. Tech. 6: 2989–3034. https://doi.org/10.5194/amt-6-2989-2013.
Lilly, D.K., Klemp, J.B., 1979. The effects of terrain shape on nonlinear hydrostatic mountain waves. J. Fluid Mech. 95, 241–261.
Meloni, D., di Sarra, A., Biavati, G., DeLuisi, J.J., Monteleone, F., Pace, G., Piacentino, S., Sferlazzo, D.M., 2007. Seasonal behavior of Saharan dust events at the Mediterranean island of Lampedusa in the period 1999–2005. Atmos. Environ. 41, 3041–3056.
Mitsakou, C., Kallos, G., Papantoniou, N., Spyrou, C., Solomos, S., Astitha, M., Housiadas, C., 2008. Saharan dust levels in Greece and received inhalation doses. Atmos. Chem. Phys. 8, 7181–7192.

Fig. 11. Path of CALIPSO and its total extinction output over Turkey (a) (Kabatas et al., 2014), WRF-Chem 30 km (b) and 10 km (c) total extinction output over Turkey along the CALIPSO path on April 14, 2008. White dashed lines show the altitude of WRF-Chem potential temperature distribution along the CALIPSO track.

Moulin, C., Lambert, C.E., Dayan, U., Masson, V., Ramonet, M., Bousquet, P., ... Dulac, F., 1998. Satellite climatology of African dust transport in the Mediterranean atmosphere. J. Geophys. Res. 103 (D11), 13,137–13,144.
Nastos, P.T., 2012. Meteorological patterns associated with intense Saharan dust outbreaks over Greece in winter. Adv. Meteorol. 828301, 17.
Nel, A., 2005. Air pollution-related illness: effects of particles. Science 308, 804–806.
Paschalidou, A., Kassomenos, P., Karanikola, P., 2015. Disaggregating the contribution of local dispersion and long-range transport to the high PM10 values measured in a Mediterranean urban environment. Sci. Total Environ. 527, 119–125.
Pierce, R.B., Schaack, T.K., Al-Saadi, J., Fairlie, T.D., Kittaka, C., Lingenfelser, G., ... Fishman, J., 2007. Chemical data assimilation estimates of continental US ozone and nitrogen budgets during INTEX-A. J. Geophys. Res. 112:D12S21. https://doi.org/10.1029/2006JD007722.
Prins, E.M., Menzel, W.P., 1994. Trends in South American biomass burning detected with the GOES VAS from 1983 to 1991. J. Geophys. Res. 99, 16,719–16,735.
Querol, X., Pey, J., Pandolfi, M., Alastuey, A., Cusack, M., Pérez, N., ... Kleanthous, S., 2009. African dust contributions to mean ambient PM10 mass-levels across the Mediterranean Basin. Atmos. Environ. 43, 4266–4277.
Rodríguez, S., Querol, X., Alastuey, A., Kallos, G., Kakaliagou, O., 2001. Saharan dust contributions to PM10 and TSP levels in Southern and Eastern Spain. Atmos. Environ. 35, 2433–2447.
Sayer, A.M., Hsu, N.C., Bettenhausen, C., Jeong, M.J., 2013. Validation and uncertainty estimates for MODIS Collection 6 "Deep Blue" aerosol data. J. Geophys. Res. 118, 7864–7872.
Sessions, W.R., Fuelberg, H.E., Kahn, R.A., Winker, D.M., 2011. An investigation of methods for injecting emissions from boreal wildfires using WRF-Chem during ARCTAS. Atmos. Chem. Phys. 11:5719–5744. https://doi.org/10.5194/acp-11-5719-2011.
Skamarock, W.C., Klemp, J.B., Dudhia, J., 2001. Prototypes for the WRF (Weather Research and Forecasting) model. Preprints, Ninth Conf. on Mesoscale Processes, Fort Lauderdale, FL. Amer. Meteor. Soc., pp. J11–J15.
Tanaka, T.Y., Chiba, M., 2006. A numerical study of the contribution of dust source regions to the global dust budget. Glob. Planet. Chang. 52, 88–104.
Tie, X., Madronich, S., Li, G.H., Ying, Z.M., Zhang, R., Garcia, A., Lee-Taylor, J., Liu, Y., 2007. Characterizations of chemical oxidants in Mexico City: a regional chemical/dynamical model (WRF-Chem) study. Atmos. Environ. 41, 1989–2008.
Tie, X., Geng, F., Guenther, A., Cao, J., Greenberg, J., Zhang, R., ... Cai, C., 2013. Megacity impacts on regional ozone formation: observations and WRFChem modeling for the MIRAGE-Shanghai field campaign. Atmos. Chem. Phys. 13:5655–5669. https://doi.org/10.5194/acp-13-5655-2013.
Winker, D.M., Hunt, W.H., McGill, M.J., 2007. Initial performance assessment of CALIOP. Geophys. Res. Lett. 34, L19803.